Journal of Analytical Atomic Spectrometry

Technical note

On-line reverse isotope dilution analysis for spatial quantification of elemental labels used in immunohistochemical assisted imaging mass spectrometry via LA-ICP-MS

Received 00th January 20xx,
Accepted 00th January 20xx

DOI: 10.1039/x0xx00000x

www.rsc.org/

David Clases[a] ,Raquel Gonzalez de Vega[a], Paul A. Adlard[b] and Philip Doble[a]

We present a novel online isotope dilution analysis (IDA) approach for the quantification of isotopically enriched metal labels used in immunohistochemical assisted imaging mass spectrometry. This technique advances recently reported online IDA for laser ablation-inductively coupled plasma mass spectrometry (LA-ICP-MS) by performing online reverse IDA of isotopically enriched elements commonly used as labels for antibodies. This approach allows relative quantification of biomolecules and is superior to other methods that have long acquisition times such as three-dimensional LA-ICP-MS, or when higher sample throughput is required. As a proof of concept, anti-tyrosine hydroxylase was labelled with Yb isotopes and incubated on two parallel cryocut sections of a mouse brain. IDA dependent parameters were determined by ablation of matrix-matched standards. Quantification by IDA was compared against external calibration and was a more robust method, unaffected by sensitivity changes originating from plasma drifts or spontaneous plasma fluctuations.

Introduction

Since the first application in 1994[1], elemental bio-imaging by LA-ICP-MS has progressed to become a routine technique for investigations of the biochemical interaction, function and fate of metals in various organisms. Recent advances and progress in metal labelling strategies for immunohistochemistry (IHC) has expanded the application of LA-ICP-MS beyond the sole investigation of the metallome towards the spatial distribution of various biomolecules. The labelling of different antibodies with different metals provides the possibility for "multi-epitope ligand cartography" of over 30 different antigens simultaneously contributing to enhanced disease diagnoses.[2]

Different labelling methods involving distinct chemistries and reagents are readily available for which MAXPAR™, MeCAT and SCN-DOTA are the most frequently used labelling agents[3]. MAXPAR™ reagents for IHC are commercially available and offer multiple binding sites for (isotopically enriched) lanthanides per antibody. This increases sensitivity significantly and results in improved contrasts and figures of merit compared to other labelling reagents.[3] Considering that higher resolutions are achievable when the sensitivity is improved makes MAXPAR™ reagents an interesting option for multiplexing and antigen detection[4].

However, in most applications, sole information about localisation of a metal species or biomolecule is not sufficient when the biological response is triggered by its concentration. Various techniques have been investigated to undertake spatial resolved calibration of metals as well as biomolecules, recently detailed and compared in several reviews [5–7]. External calibration using matrix-matched laboratory standards has been applied most frequently [8–11]. With the aim to mimic the biological environment and to guarantee comparable physical and chemical behaviours in terms of ablation and ionisation characteristics, different materials have been suggested for the fabrication of matrix-matched standards including gelatin or an homogenate of a target organ such as breast or brain tissue spiked with the element of interest [8,12–14]. Other quantification strategies use internal standardisation or isotope dilution analysis (IDA).[15,16]

Nevertheless, the absolute quantification of biomolecules with IHC and LA-ICP-MS remains challenging since multiple factors such as coverage, affinity of the antibody to the antigen, labelling degrees as well as wash-out effects must be considered to obtain truly quantitative results[17,18]. Therefore, the quantification of the metal label allows relative comparisons of samples under investigation, which is sufficient for many biological applications[19].

Compared to external calibration, IDA offers generally higher accuracy and precision as the isotope ratio remains constant, even during instrumental drifts or spontaneous plasma fluctuations. Limbeck et al. and Bonta et al. demonstrated how rapid instrumental drift may occur.[20,21] They found a decline of up to 25% sensitivity after short time intervals or after the ablation of small sample sets. To compensate for sensitivity

[a] Elemental Bio-Imaging Facility, University of Technology Sydney, Sydney, NSW, Australia.
[b] The Florey Institute of Neuroscience and Mental Health, Parkville, Victoria, Australia.

drift, internal standards may be used directly on the sample to compensate both drifts in LA and ICP-MS instrumentation.[12,14,21] Recent literature describes coating or blending strategies to cover or mix the sample with an enriched isotope spike[22,23]. However, higher spatial resolution is limited by this coating/blending approach due to a lack of homogeneity. Another approach is to use a "post-laser" stable isotope enriched spike. Fernandez *et al*. introduced an on-line IDA approach for LA-ICP-MS in 2014, where sequential ablation of SRMs and samples in combination with an isotope enriched "post-laser" aerosol spike, allowed calculation of important IDA parameters such as the mass fraction [16,24]. This is a valid method if the standard and sample have identical matrix compositions. However, this is particularly difficult to maintain when analysing biological tissues. Douglas *et al.* [25] presented a systematic approach to estimate the uncertainty generated when analysing biological tissues and a method to measure the mass flow rate directly. They found that uncertainty was reduced by up to two times compared to external calibration. Bauer *et al.*[26] recently performed online IDA employing Pt spiked gelatin as a matrix-matched standard to perform the spatial quantification of perfused platinum in biological tissue.

IDA has not been used for IHC assisted multiplexing analysis by LA-ICP-MS, despite the desirable characteristic of isotopic enrichment in the labelling metal reagents such as using MAXPAR™. Therefore, naturally abundant post-laser spike solutions can be employed to perform quantification of labelled metals by online reverse IDA. Compared against external calibration, IDA promises improved accuracy, precision, speed and compensation of instrumental drifts likely to occur when long measurements are undertaken.

In this work, we expand the application of on-line IDA to the application of IHC-assisted LA-ICP-MS with on-line reverse IDA for the quantification of metals labels. For a proof of concept, anti-tyrosine hydroxylase was labelled with Yb isotopes and incubated on mouse brain sections. To demonstrate the benefits in terms of signal stability important during long acquisitions or in three-dimensional imaging, results were compared to data obtained by external calibration.

Experimental

Chemicals and consumables

For the IHC staining process, anti-tyrosine hydroxylase was purchased from In vitro Technologies (Victoria, Australia) and a ^{172}Yb MAXPAR™ labelling kit from Millennium Science (Victoria, Australia). The following reagents and consumable were all obtained from Sigma Aldrich (Darmstadt, Germany). For filtration, centrifugal filters with mass cut offs at 3 kDa and 50 kDa were used (Amicon® Ultra-0.5). All containers to store and dilute reagents were made of polypropylene to prevent adsorption effects. Paraformaldehyde was used for the post fixation of the biological tissue. An antigen unspecific blocking solution was composed of 500 µl of 20 % BSA, 300 µl of 10 % TritonX, 300 µl of normal goat serum and 8.9 ml of PBS. High purity gelatin from bovine skin was used to manufacture a solid Yb containing matrix matched standard. The gelatin (100 mg) was mixed with 900 µL of spike solution, heated to 55 ºC and then filled into wells (HybriWell™, 50 µL, 9.8mm x 20 mm x 0.25 mm). Various Yb standards (10, 50, 100, 500, 1000 ng/g) were prepared to investigate the influence of the standard concentration on the calibration result. For the on-line reverse IDA spike solution, an Yb ICP-MS calibration standard containing natural abundant Yb was obtained in 2 % HNO_3 from High Purity Standards (SC, USA) and diluted in 2 % aqueous nitric acid (67-69 % (w/w), Seastar Chemicals Inc., BC, Canada) to an approximate concentration of 0.5 µg/L. The flow rate was set to approximately 0.5 mL/min and aspirated via a concentric nebuliser. Water was obtained from an arium® pro system (Sartorius Stedim Plastics GmbH, Germany). The detectors dead-time was determined using a Lu ICP-MS standard (10 µg/g in 2 % HNO_3, High Purity Standards) and subsequently compensated by the software.

Sample preparation

All animal experiments/tissue collections were approved by the Howard Florey Animal Ethics Committee and were conducted in accordance with the Australian Code of Practice for the Care and Use of Animals for Scientific Purposes as described by the National Health and Medical Research Council of Australia. All animals had free access to food and water and were group-housed in individually ventilated cages in The Florey Institute Animal Facility under controlled temperature (22±2˚C) and lighting (14:10 hours light/dark cycle) conditions.

The antibody labelling was carried out by reducing it and conjugating a metal loaded polymer to the F_c region. This was accomplished following the standard Fluidigm protocol carefully (PRD 002, Version 10). Wild type C57Bl/6 mouse brain tissue was fixed with 2 % paraformaldehyde for 5 minutes and subsequently equilibrated in PBS. The blocking solution containing BSA was applied for 35 minutes. After washing the tissue, the labelled antibody solution was then incubated on the sections which were left overnight before washing and air drying the specimen.

The isotopic enriched Yb as well as the natural abundant Yb ICP-MS calibration solution were diluted in 2 % aqueous nitric acid to characterise their isotope abundance by ICP-MS, which rendered it unnecessary to compensate for mass bias effects during IDA.

Douglas et al. showed previously that the analyte ratios in sample and calibration standard require careful consideration as they impact accuracy [25]. Therefore, six gelatin standards containing different concentrations of ^{172}Yb (0 µg/L, 10 µg/L, 50 µg/L, 100 µg/L, 500 µg/L, 1000 µg/L) were prepared to determine the constant values in IDA. To compare online IDA with external calibration, six external Yb gelatin standards (natural Yb abundance) were prepared as mentioned before (15, 73, 240, 700, 1350 µg/L). The exact Yb concentrations of the standards were determined after digestion in aqueous nitric acid and external calibration by standard ICP-MS, respectively.

Instrumentation and experimental parameters

All analyses were carried out employing an iCAP™ RQ quadrupole ICP-MS (Thermo Fisher Scientific, Bremen, Germany) equipped with nickel sampler and skimmer and operated with Qtegra™ software (Version 2.7.2425.65). Measurements were conducted using the following conditions: A PFA MicroFlow nebuliser (Elemental Scientific, Omaha, NE) was used in combination with a cyclonic spray chamber (2.7 °C, Glass Expansion, Victoria, Australia) for wet aerosol generation. The measurements were carried out using the following plasma parameters: RF power, 1550 W, coolant gas flow, 14 L/min; auxiliary gas flow, 0.9 L/min, nebuliser gas flow, 0.9 L/min. For sample and spike characterization, ^{168}Yb, ^{170}Yb, ^{171}Yb, ^{172}Yb, ^{173}Yb, ^{174}Yb, ^{176}Yb were analysed with a dwell time of 70 ms. Among other biological relevant elements, the ratio of ^{172}Yb and ^{173}Yb was measured with a 70 ms dwell time. As laser ablation system an LSX-213 G2+ from Teledyne CETAC Technologies (Omaha, NE, USA) was operated with an "aerosol rapid introduction system" (ARIS, Teledyne CETAC Technologies). Line-by-line scans were performed. The laser beam spot size was adjusted to 30 µm, the scan speed to 120 µm/s and the frequency to 20 Hz generating a fluence of 3.48 J/cm^2. The quadrupoles integration time (0.25 s) was set to produce square voxels (30x30 µm). Helium was used as carrier gas with a flow rate of 0.4 L/min (0.25 L/min cell gas, 0.15 L/min ablation cup gas.

Results and discussion

MAXPAR™ protocols employ enriched isotopes to routinely perform cytometry and facilitates quantification by IDA as no further enriched elements are necessary. Instead, conventional ICP-MS standard solutions may be used as the spike solution when conducting reverse IDA. The isotopic ratio in each voxel of an image can be converted by the common IDA equation (1) into a concentration.

$$c_S = c_{Sp}\frac{m_{Sp}}{m_S}\frac{M_s}{M_{Sp}}\frac{A^b_{Sp}}{A^a_S}\left(\frac{R_m - R_{Sp}}{1 - R_m \cdot R_S}\right) \qquad (1)$$

where c is the concentration, m the mass, M the molar mass and A the abundance of a selected isotope (a, b) in the sample (S) or the spike (Sp), respectively. R_m is the measured ratio of two isotopes and R_S as well as R_{Sp} are defined as $R_s = A^S_b/A^S_a$ and $R_{sp} = A^{Sp}_a/A^{Sp}_b$, respectively. Since MAXPAR™ lanthanides were not intended to be exploited for direct quantification, parameters such as concentration or abundance are usually not provided or roughly estimated. Therefore, abundances and concentrations must be determined accurately for IDA. Conventional liquid introduction based ICP-MS, yielded in the total Yb concentration at 1910 mg/L, and an enrichment of 94.7% for ^{172}Yb. The determined abundance is shown in Figure 1 and compared against the natural abundance.

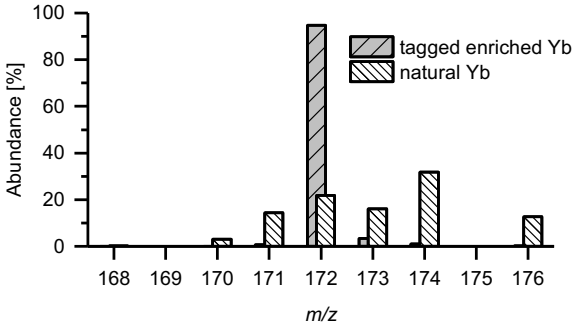

Figure 1: Comparison of the natural abundance and the abundance of enriched Yb used in MAXPARTM reagents.

The parameters m_S and m_{Sp}, which represent the masses of the dry aerosol originating from the ablation process and of the wet nebulised aerosol being mixed, respectively, cannot be determined individually. Ideally, these two parameters remain constant during analysis for the determination of the mass fraction when a sample and a standard are investigated sequentially [16]. However, it must be emphasised that the heterogeneous environment of biological tissues puts the suitability of a homogenous matrix-matched standard in question. It is likely that structural features with different densities and therefore different aerosol characteristics, cannot be mimicked precisely. Differences between standard and sample matrices potentially result in variable results and must be considered carefully when reporting quantified data[25,27]. Nonetheless, this problem also applies to external calibration using matrix matched standards.

Assuming consistent ablation characteristics, all constant parameters including the mass fraction, the concentration of the spike aerosol, the molecular masses as well as the isotope abundances can be summarised in a collective constant K and its value can be calculated by ablating a solid matrix matched standard with a known concentration $c_{standard}$ as shown in equation (2).

$$K = c_{wet\ spike}\frac{m_{Sp}}{m_S}\frac{M_s}{M_{Sp}}\frac{A^b_{Sp}}{A^s_a} = c_{standard}\left(\frac{R_m - R_{Sp}}{1 - R_m \cdot R_S}\right)^{-1} \qquad (2)$$

Finally, the concentration within a sample can be calculated using equation (3).

$$c_S = K\left(\frac{R_m - R_{Sp}}{1 - R_m \cdot R_S}\right) \qquad (3)$$

The measured value of K deviated by 12.3 % when measured with standards of Yb of 10, 50, 100, 500, 1000 ng/g. This variation was predominantly a consequence of typical standard deviations in LA-ICP-MS measurements, which are approximately 10%.

One of the crucial advantages of IDA is its capability to overcome any type of drift occurring after the sample and spike solution have mixed. This includes plasma drifts or drifts associated with material deposition on interface compartments of the two-staged vacuum interface of any ICP-MS system. Such drifts become increasingly important when analysing large samples or when performing three-dimensional imaging, which

require many hours or even several days of acquisition. To demonstrate the advantages of IDA over commonly applied external calibration, both were compared, and a signal drift was induced artificially. As a model system, tyrosine hydroxylase, an enzyme primarily located in substantia nigra and crucial for the formation of dopamine[28] was incubated with a polyclonal antibody labelled with ^{172}Yb. Therefore, the Yb concentration acted as a proxy target for the abundance of tyrosine hydroxylase and relative quantification. Figure 2 illustrates the quantitative ^{172}Yb distribution calibrated by IDA (Fig. 2(a)) and external calibration (Fig 2 (b)). Line scans were performed from left to right starting at the bottom. The ICP-MS sensitivity was altered halfway through the analysis (approximately 50 %) to simulate drift/fluctuation (indicated by the dotted yellow line). External calibration did not provide accurate concentrations once the sensitivity was altered. On the other hand, the quantification by IDA was unaffected demonstrating that sensitivity-independent isotope ratios allowed robust quantification even after the sensitivity had dropped dramatically. For comparison of IDA and external calibration quantification, the isotopic ratios of ^{172}Yb and ^{173}Yb were recorded for IDA, whilst the constant signal of the wet spike aerosol was subtracted for external calibration. This approach increased the standard deviation of low Yb concentrations determined by external calibration, and was visible as inconsistencies between both calibrated images at low Yb concentrations (violet). However, higher concentrations in the target area of the substantia nigra remained unaffected for both IDA and external calibration before the sensitivity change was induced.

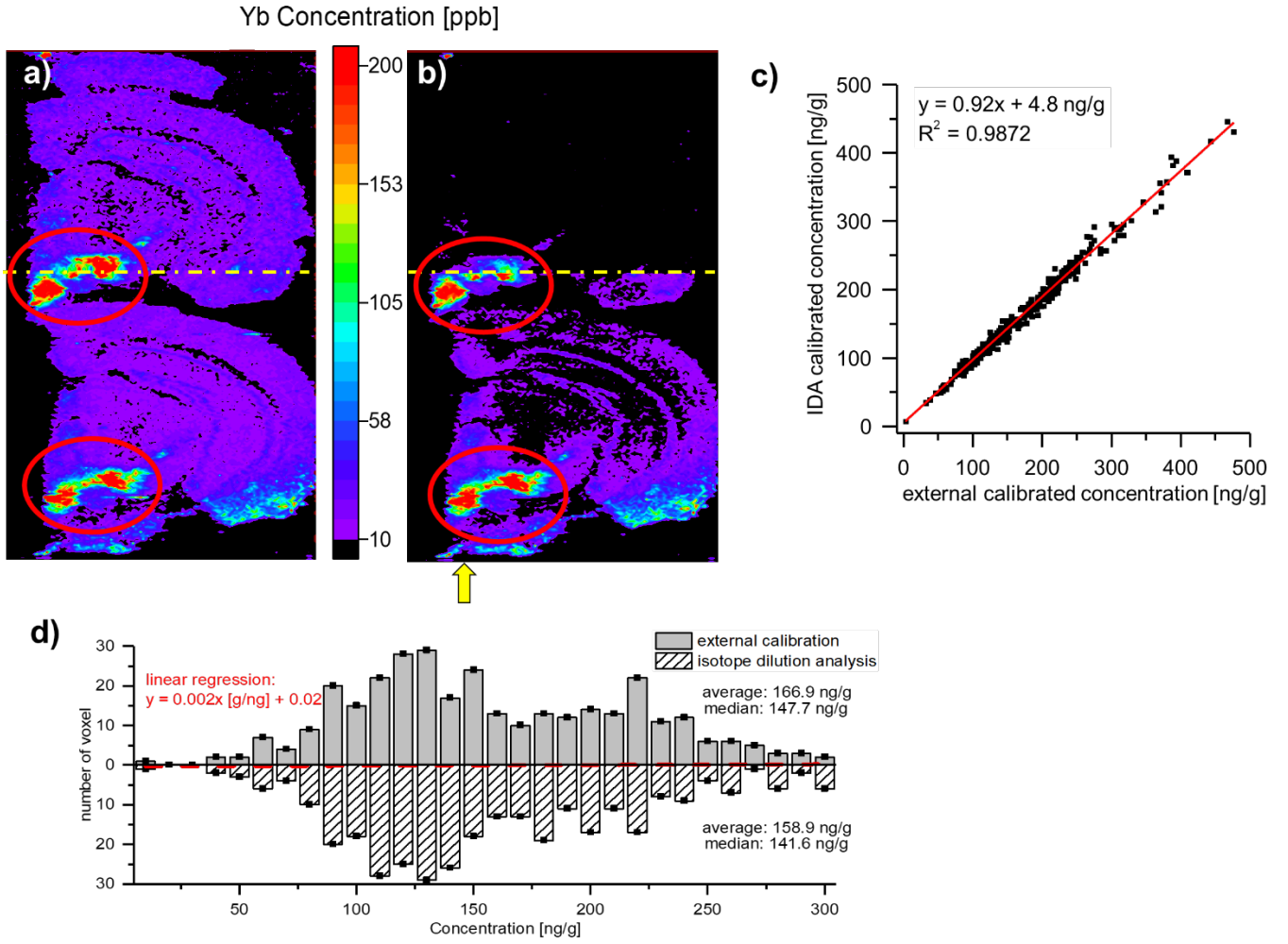

Figure 2. Comparison of the Yb calibration by IDA **(a)** and by external calibration **(b)** employing LA-ICP-MS of two parallel sections of a mouse brain. The yellow line indicates an intentionally induced sensitivity shift to simulate the effect of sensitivity loss during long time acquisitions. The red ovals show the area of interest, the substantia nigra. IDA was not affected by the induced sensitivity change, whereas external calibration was substantially affected. **(c)**: Correlation of Yb concentration levels the substantia nigra determined by IDA and external calibration, respectively. **(d)**: Histogram of the concentrations of all voxels located within the substantia nigra. Similar results can be seen for both external calibration (top) and IDA (bottom), respectively. External calibration yielded an average value of 166.9 ng/g (median 147.7 ng/g), and IDA 158.9 ng/g (median 141.6 ng/g). The red line depicts the correlation between external calibration and IDA and the influence of low and high Yb levels on the calibration within the substantia nigra.

Although low concentrations of Yb were compromised by the mathematical correction, it needs to be emphasised that the affected areas were due to non-specific bindings of the primary antibody, which is unavoidable using standard immunohistochemical techniques. This background staining was not relevant to the expression of the protein in the target area of the substantia nigra and was of little consequence for this application. The substantia nigra is clearly visible as Yb hotspot corresponding to the tyrosine hydroxylase distribution (indicated with a red oval). Figure 2 (a) and (b) illustrate that both external calibration and IDA report similar Yb concentrations within this region of interest with unaltered sensitivity (below the yellow line). The alteration of sensitivity (above the yellow line) induced a systematic error for external quantification which cannot be corrected without recalibration. Isotope ratios, however, were not affected.

Figure 2 (c) shows the concentration correlation of both calibration approaches in the substantia nigra before sensitivity alteration with an R^2 value of 0.9872, a slope of 0.92 and an intercept of 4.8 ng/g. The deviation from an ideal value of 1 and 0 ng/g was in part due to the subtraction of the IDA spike solution intensity from the external calibration data (9890 ± 430 counts/s; equivalent to 34.4 ± 7 ng/g).

Figure 2 (d) shows a histogram of the voxel concentration across the substantia nigra with an interval of 15 ng/g. It compares the concentrations obtained by IDA (bottom) and external calibration (top), respectively, and demonstrates a similar quantitative distribution for both calibration methods with unaltered sensitivity. The average value for external calibration was 166.9 ng/g (median 147.7 ng/g) and 158.9 ng/g (median 147.7 ng/g) for IDA, respectively. The red line depicts a linear regression over all data points showing a negligible quantitative bias between low and high concentrations. This similarity of IDA and external calibration demonstrates that IDA was a viable quantification strategy, and the mathematical correction had negligible consequences within the area of interest.

Conclusions

This work demonstrated a new approach for online IDA for the quantification of elemental labels routinely used for IHC staining protocols. These protocols utilised enriched isotopes typically used for mass cytometry, allowing quantification by IDA in which the sample aerosol is mixed with a wet lanthanide aerosol with a natural isotopic abundance. To calculate mass flow parameters, a ^{172}Yb spiked matrix-matched standard was ablated prior to analysing the brain sections. Both external calibration and IDA methods utilised gelatin for matrix matching allowing general comparisons of high concentration distributions and robustness. IDA was the more robust quantification method compared to external calibration, as isotope ratios were not influenced by signal drifts or plasma fluctuations caused by events taking place after sample and spike mixing. IDA therefore compensated not only plasma drifts but also losses of sensitivity associated with material deposition at the interface and signal fluctuations caused by ICP-MS. This becomes particularly relevant when long measurements of several hours or even days, such as for three dimensional elemental bioimaging.[28] This makes online reverse IDA a promising technique for the quantitative evaluation of metals used in IHC and therefore relative quantification of biomolecules.

Conflicts of interest

There are no conflicts to declare.

Acknowledgements

D.C. is funded by the Deutsche Forschungsgemeinschaft (DFG. German Research Foundation) – 417283954.
P.A.D. and P.A.A. are the recipients of an Australian Research Council Discovery Project (DP170100036). The Florey Institute of Neuroscience and Mental Health acknowledge the strong support from the Victorian Government and in particular the funding from the Operational Infrastructure Support Grant.

References

1 S. Wang, R. Brown and D. J. Gray, *Appl. Spectrosc.*, 1994, **48**, 1321–1325.
2 C. Giesen, H. A. Wang, D. Schapiro, N. Zivanovic, A. Jacobs, B. Hattendorf, P. J. Schüffler, D. Grolimund, J. M. Buhmann, S. Brandt, Z. Varga, P. J. Wild, D. Günther and B. Bodenmiller, *Nat. Methods*, 2014, **11**, 417.
3 L. Waentig, N. Jakubowski, S. Hardt, C. Scheler, P. H. Roos and M. W. Linscheid, *J. Anal. At. Spectrom.*, 2012, **27**, 1311.
4 J. Lear, D. J. Hare, F. Fryer, P. A. Adlard, D. I. Finkelstein and P. A. Doble, *Anal. Chem.*, 2012, **84**, 6707–6714.
5 I. Konz, B. Fernández, M. L. Fernández, R. Pereiro and A. Sanz-Medel, *Anal. Bioanal. Chem.*, 2012, **403**, 2113–2125.
6 D. Hare, C. Austin and P. Doble, *Analyst*, 2012, **137**, 1527–1537.
7 D. Kretschy, G. Koellensperger and S. Hann, *Anal. Chim. Acta*, 2012, **750**, 98–110.
8 D. J. Hare, J. Lear, D. Bishop, A. Beavis and P. A. Doble, *Anal. Methods*, 2013, **5**, 1915–1921.
9 M. Arora, D. Hare, C. Austin, D. R. Smith and P. Doble, *Sci. Total Environ.*, 2011, **409**, 1315–1319.
10 D. Hare, C. Austin, P. Doble and M. Arora, *J. Dent.*, 2011, **39**, 397–403.
11 D. J. Hare, E. P. Raven, B. R. Roberts, M. Bogeski, S. D. Portbury, C. A. McLean, C. L. Masters, J. R. Connor, A. I. Bush, P. J. Crouch and P. A. Doble, *Neuroimage*, 2016, **137**, 124–131.
12 R. González de Vega, M. L. Fernández-Sánchez, J. Pisonero, N. Eiró, F. J. Vizoso and A. Sanz-Medel, *J. Anal. At. Spectrom.*, 2017, **32**, 671–677.
13 K. Jurowski, M. Szewczyk, W. Piekoszewski, M. Herman, B. Szewczyk, G. Nowak, S. Walas, N. Miliszkiewicz, A. Tobiasz and J. Dobrowolska-Iwanek, *J. Anal. At. Spectrom.*, 2014, **29**, 1425–1431.
14 J. O'Reilly, D. Douglas, J. Braybrook, P.-W. So, E. Vergucht, J. Garrevoet, B. Vekemans, L. Vincze and H. Goenaga-Infante, *J. Anal. At. Spectrom.*, 2014, **29**, 1378.
15 D. Pozebon, G. L. Scheffler, V. L. Dressler and M. A. G. Nunes, *J. Anal. At. Spectrom.*, 2014, **29**, 2204–2228.
16 B. Fernández, P. Rodríguez-González, J. I. García Alonso, J. Malherbe, S. García-Fonseca, R. Pereiro and A. Sanz-Medel, *Anal. Chim. Acta*, 2014, **851**, 64–71.
17 A. R. Dixon, C. Bathany, M. Tsuei, J. White, K. F. Barald and S. Takayama, *Expert Rev. Mol. Diagn.*, 2015, **15**, 1171–86.
18 G. Schwarz, L. Mueller, S. Beck and M. W. Linscheid, *J. Anal. At. Spectrom.*, 2014, **29**, 221–233.
19 S. E. Ong and M. Mann, *Nat. Chem. Biol.*, 2005, **1**, 252–262.
20 A. Limbeck, P. Galler, M. Bonta, G. Bauer, W. Nischkauer and F. Vanhaecke, *Anal. Bioanal. Chem.*, 2015, **407**, 6593–6617.
21 M. Bonta and H. Lohninger, *Analyst*, 2014, **139**, 1521–31.
22 M. Tibi and K. G. Heumann, *J. Anal. At. Spectrom.*, 2003, **18**, 1076–1081.
23 L. Feng, J. Wang, H. Li, X. Luo and J. Li, *Anal. Chim. Acta*, 2017, **984**, 66–75.
24 C. Pickhardt, A. V Izmer, M. V Zoriy, D. Schaumlöffel and J. Sabine Becker, *Int. J. Mass Spectrom.*, 2006, **248**, 136–141.
25 D. N. Douglas, J. O'Reilly, C. O'Connor, B. L. Sharp and H. Goenaga-Infante, *J. Anal. At. Spectrom.*, 2016, **31**, 270–279.
26 O. B. Bauer, C. Köppen, M. Sperling, H.-J. Schurek, G. Ciarimboli and U. Karst, *Anal. Chem.*, 2018, **90**, 7033–7039.
27 B. Fernández, P. Rodríguez-González, J. I. García Alonso, J. Malherbe, S. García-Fonseca, R. Pereiro and A. Sanz-Medel, *Anal. Chim. Acta*, 2014, **851**, 64–71.
28 B. Paul, D. J. Hare, D. P. Bishop, C. Paton, V. T. Nguyen, N. Cole, M. M. Niedwiecki, E. Andreozzi, A. Vais, J. L. Billings, L. Bray, A. I. Bush, G. Mccoll, B. R. Roberts, P. A. Adlard, D. I. Finkelstein, J. Hellstrom, J. M. Hergt, J. D. Woodhead and P. A. Doble, *Chem. Sci.*, 2015, **6**, 5383–5393.

